BJP BRITISH JOURNAL OF PHARMACOLOGY

BPS BRITISH PHARMACOLOGICAL SOCIETY

British Journal of Pharmacology (2010), 160, 747–761

0007-1188/10
www.brjpharmacol.org

THEMED ISSUE: CANNABINOIDS

RESEARCH PAPER

Neuroprotective potential of CB_1 receptor agonists in an *in vitro* model of Huntington's disease

EL Scotter[1], CE Goodfellow[1], ES Graham[1], M Dragunow[1,2] and M Glass[1]

[1]*Department of Pharmacology and Clinical Pharmacology, Faculty of Medical and Health Sciences, University of Auckland, Grafton, Auckland, New Zealand, and* [2]*National Research Centre for Growth and Development, Faculty of Medical and Health Sciences, University of Auckland, Grafton, Auckland, New Zealand*

Background and purpose: The therapeutic potential of cannabinoids in Huntington's disease (HD) has been investigated by several groups with complex and sometimes contrasting results. We sought to examine key points of intersection between cannabinoid receptor 1 (CB_1) signalling, survival and the formation of mutant huntingtin aggregates in HD.
Experimental approach: Using a simplified pheochromocytoma (PC12) cell model of HD expressing exon 1 of wild-type or mutant huntingtin, we assayed cell death and aggregate formation using high-throughput cytotoxicity and image-based assays respectively.
Key results: CB_1 activation by HU210 conferred a small but significant level of protection against mutant huntingtin-induced cell death. *Pertussis* toxin uncoupled HU210 from the inhibition of cAMP, preventing rescue of cell death. Phosphorylation of extracellular signal-regulated kinase (ERK) was also critical to CB_1-mediated rescue. Conversely, treatments that elevated cAMP exacerbated mutant huntingtin-induced cell death. Despite opposing effects on HD cell survival, both HU210 and compounds that elevated cAMP increased the formation of mutant huntingtin aggregates. The increase in aggregation by HU210 was insensitive to *Pertussis* toxin and UO126, suggesting a G-protein alpha subtype s (G_s)-linked mechanism.
Conclusions and implications: We suggest that the CB_1 receptor, through G-protein alpha subtype i/o ($G_{i/o}$)-linked, ERK-dependent signal transduction, is a therapeutic target in HD. However the protective potential of CB_1 may be limited by promiscuous coupling to G_s, the stimulation of cAMP formation and increased aggregate formation. This may underpin the poor therapeutic efficacy of cannabinoids in more complex model systems and suggest that therapies that are selective for the $G_{i/o}$, ERK pathway may be of most benefit in HD.
British Journal of Pharmacology (2010) **160,** 747–761; doi:10.1111/j.1476-5381.2010.00773.x
This article is part of a themed issue on Cannabinoids. To view the editorial for this themed issue visit http://dx.doi.org/10.1111/j.1476-5381.2010.00831.x

Keywords: Huntington's disease; CB_1; cannabinoid; huntingtin; aggregate; neuroprotection; ERK

Abbreviations: BSA, bovine serum albumin; CB_1, cannabinoid receptor 1; D1, dopamine receptor 1; D2, dopamine receptor 2; ERK, extracellular signal-regulated kinase; $G_{i/o}$, G-protein alpha subtype i/o; G_s, G-protein alpha subtype s; HD, Huntington's disease; PC12, pheochromocytoma; PKA, protein kinase A; PTX, *Pertussis* toxin; SFM, serum-free media; SFM/BSA, serum-free media with BSA; TFZ, tebufenozide

Introduction

Huntington's disease (HD) is a hereditary neurodegenerative disorder in which polyglutamine repeat expansion in the huntingtin protein leads to its abnormal aggregation and, through ill-defined mechanisms, subsequent neuronal cell death (reviewed in Ross and Margolis, 2001). The cortex and the basal ganglia, comprising the striatum (caudate nucleus and putamen), globus pallidus, substantia nigra and subthalamic nucleus, are the brain regions affected earliest and most severely in HD. In the HD striatum, there is selective degeneration of the GABAergic medium spiny neurons and relative sparing of aspiny interneurons (Ferrante *et al.*, 1985; Graveland *et al.*, 1985). One of the first detectable signs of cellular dysfunction in striatal medium spiny neurons in HD is the loss of CB_1 cannabinoid G-protein-coupled receptors (GPCRs) from terminals and somata (Glass *et al.*, 2000). There is a

Correspondence: Associate Professor Michelle Glass, Centre for Brain Research and Department of Pharmacology, University of Auckland, Private Bag 92019, Auckland, New Zealand. E-mail: m.glass@auckland.ac.nz
Received 25 November 2009; revised 4 March 2010; accepted 6 March 2010

significant decrease in CB_1 density in the internal segment of the globus pallidus in the absence of significant cell death and prior to changes in co-localized receptors (Glass *et al*., 2000). This suggests that CB_1 loss may represent an early marker of neuronal dysfunction in HD.

The loss of CB_1 may also further exacerbate neuronal injury in HD. In transgenic (R6/1) HD mice, an environmental enrichment paradigm that enhanced CB_1 expression was able to delay the progression of symptoms and restore the deficit of brain-derived neurotrophic factor (van Dellen *et al*., 2000; Glass *et al*., 2004; Spires *et al*., 2004). Fibroblast growth factor 2 treatment of R6/2 mice has also revealed a correlation between CB_1 up-regulation and prolonged survival (Jin *et al*., 2005). Together these data present the possibility that activation of CB_1 may be therapeutic in HD. However, most studies seeking to directly explore the neuroprotective benefit of augmenting CB_1 signalling in HD have used toxin models of the disease and have been conflicting as to the receptor's usefulness (Lastres-Becker *et al*., 2003a,b).

The influence of cannabinoid therapy on huntingtin aggregation has yet to be investigated directly. Huntingtin aggregation is likely to have a key role in the neurodegenerative process in HD, as the critical repeat length for spontaneous aggregation of polyglutamines (37 repeats) corresponds closely with the minimum repeat length for the development of HD (Chen *et al*., 2001). While inhibitors of mutant huntingtin aggregation have shown therapeutic benefit both *in vivo* and *in vitro* (Lehrach and Wanker, 2001; Sanchez *et al*., 2003), it remains to be established whether it is the soluble oligomers or the insoluble fibrils/aggregates of mutant huntingtin which are the key neurotoxic species. Mature aggregates may be considered a marker of the various possible toxic conformers, and as such may provide useful insights into pathways modulated by therapeutics, including cannabinoids.

Our findings in a pheochromocytoma (PC12) cell model of HD support a mechanism for neuroprotection via CB_1 coupled to G-protein alpha subtype i/o ($G_{i/o}$) and the phosphorylation of extracellular signal-regulated kinase (ERK). However, coupling of CB_1 to G-protein alpha subtype s (G_s) G-protein enhanced the formation of mutant huntingtin aggregates, which were associated with cell death. These findings suggest that the loss of $G_{i/o}$-linked CB_1 signalling early in HD may enhance neuronal vulnerability to the primary disease process, and that agonists of GPCRs that couple only to $G_{i/o}$ may be of therapeutic benefit in HD.

Methods

Cell culture and plasmid constructs

The *in vitro* HD model used for this study was a PC12 cell line that expresses N-terminal huntingtin protein in response to induction with the insect steroid hormone tebufenozide (TFZ) (Aiken *et al*., 2004). The huntingtin construct had been cloned into the TFZ-inducible plasmid pBWN (Suhr *et al*., 1998) and encodes the first 67 amino acids with a polyglutamine tract of 25 (wild-type) or 97 (mutant) repeats and a C-terminal enhanced green fluorescent protein (EGFP) tag (Kazantsev *et al*., 1999). This cell line was kindly gifted to us by Dr Eric Schweitzer (Brain Research Institute, UCLA, Los Angeles, CA, USA). Clonal populations of each of these lines (PC12 25Q/97Q) were stably transfected with HA-tagged human CB_1 (PC12 25Q CB_1/97Q CB_1) or dopamine receptor 1 (PC12 25Q D1/97Q D1) constructs, under constitutive promotion in the plasmid pEF4a His V5A (Invitrogen, Carlsbad, CA, USA) [Receptor nomenclature conforms to Alexander *et al*. (2008)]. Receptor constructs were generated by KpnI/PmeI (CB_1) or KpnI/XbaI (D1) restriction digest of HA-tagged receptor sequences from pcDNA 3.1(+) constructs purchased from the Missouri S & T cDNA Resource Centre (Rolla, MO, USA) (catalogue numbers: #CNR01LTN00 and #DRD010TN00), and ligation into KpnI/PmeI- or KpnI/XbaI-digested pEF4a His V5A.

Cells were cultured in Dulbecco's modified Eagle's medium (DMEM, Invitrogen) containing high glucose (4500 $mg{\cdot}L^{-1}$), L-glutamine (4 mM) and sodium pyruvate (110 $mg{\cdot}L^{-1}$) and supplemented with 10% (v/v) horse serum, 5% (v/v) fetal bovine serum, 100 $units{\cdot}mL^{-1}$ penicillin, 100 $\mu g{\cdot}mL^{-1}$ streptomycin, 25 mM HEPES and 250 $\mu g{\cdot}mL^{-1}$ geneticin. Also, 500 $\mu g{\cdot}mL^{-1}$ zeocin was added for receptor-transfected lines. Cells were grown at 37°C in a humidified 95% air, 5% CO_2 environment.

Reverse transcriptase PCR

Endogenous GPCR expression in PC12 cells compared with CBB6 (CBAxC57/B6) mouse cerebellum (kindly gifted by Associate Professor Anthony Hannan, Howard Florey Institute, Melbourne, Vic., Australia) was examined using reverse transcriptase PCR. One million cells or <100 mg fresh frozen mouse cerebellum ($n = 3$ animals) were homogenized in 1 mL TRIzol reagent (Invitrogen) on ice and total RNA extracted as per manufacturer's directions. Two micrograms of RNA was DNase-treated and cDNA was generated using Superscript II reverse transcriptase (Invitrogen) and according to manufacturer's instructions. Receptor PCR was performed using 1 µL cDNA generated as above, 1 µM forward and reverse primers, 160 µM dNTPs and 0.5 U Taq DNA polymerase (buffered, Roche, Basel, Switzerland) in a GeneAmp PCR system 9700 (Applied Biosystems Inc., Foster City, CA, USA). Cycling conditions were as follows: 94°C, 2 min; (94°C, 15 s; annealing temp, 30 s; 72°C, extend time) × 35 (CB_1, D2, β-actin) or 40 (D1) cycles; 72°C, 7 min.

Where annealing temp: CB_1 = 58°C; D1 = 63°C; D2 = 60°C; β-actin = 60°C and extend time: CB_1 = 90 s; D1 = 70 s; D2 = 30 s; β-actin = 30 s. Forward and reverse primer sequences were: CB_1: atgaagtcgatcctagatggccttgcaga, tcacagagcctcggcagacgtg (previously validated to amplify endogenous mouse CB_1 (Graham *et al*., 2006), rat CB1, and human CB1 in brain samples and transfected cell lines (data not shown); D1: ggtccaaggtgacca acttct, accgtctctatggcattattcgt; D2: ctggagaggcagaactggag, ggagatggtgaaggacagga; B-actin: gctcgtcgtcgacaacggctc, caaacatgatctgggtcatcttctc. GPCR primers were designed against regions of high identity between rat and human sequences in order to detect both endogenous and transfected receptor simultaneously. Thirty-five to forty cycles of PCR were used to aid detection of endogenous receptors even if expressed at low levels.

[^{3}H]-SR141716A binding assay

To investigate endogenous CB_1 receptor expression and measure transfected CB_1 receptor expression levels, whole cell

binding was performed as described previously (Saidak *et al*., 2006) but with modifications. Briefly, PC12 cells were plated at 150 000 cells·well^{-1} in poly-L-lysine-coated 24-well plates and allowed to adhere overnight. Cells were washed in assay buffer [DMEM, 25 mM HEPES pH 7.4, 5 mg·mL^{-1} bovine serum albumin (BSA)] and incubated at 37°C for 1 h with 5 nM [^{3}H]-SR141716A (two batches used with specific activity of 55 μCi·mol^{-1} and 50 μCi·mol^{-1}, respectively, Amersham, Chalfont St. Giles, UK). Non-specific binding was defined by inclusion of 100 nM SR141716A in the incubation. Cells were then placed on ice, washed twice with 1 mL assay buffer and lysed in 250 μL 0.1 M NaOH for 1 h at room temperature. A total of 200 μL·well^{-1} lysate was taken into 4 mL scintillation vials (Perkin-Elmer, Waltham, MA, USA) and 2 mL scintillant (Starscint, Packard Bioscience, Meriden, CT, USA) added. Vials were shaken, allowed to disperse overnight, and counted for 2 min·well^{-1} on a Wallac 1450 Microbeta Jet Trilux Scintillation Counter (Perkin-Elmer). Total protein per well was determined by Bio-Rad DC Protein Assay (Bio-Rad Laboratories, Hercules, CA, USA) of 5 μL of the lysate. Values are expressed as femtomoles of radioligand bound per milligram of cells.

Imaging receptor localization

In order to confirm that transfected CB_1 and D1 receptors were appropriately localized to the cell surface, PC12 cell lines were labelled using a live-cell method described previously (Grimsey *et al*., 2008). Briefly, for cell surface receptor labelling, culture medium was replaced with serum-free media with 5 mg·mL^{-1} BSA (SFM/BSA) with mouse α-HA.11 antibody (Covance, Princeton, NJ, USA) at 1:500 dilution for 30 min at room temperature with rocking. Unbound antibody was removed by 1× wash in fresh SFM/BSA. Cells were then fixed in 4% paraformaldehyde for 10 min and washed in phosphate-buffered saline (PBS) for 2 × 10 min. Secondary antibody labelling was performed post fixation using Alexa 594 goat α-mouse antibody (Molecular Probes, Eugene, OR, USA) at 1:400 in immunobuffer with Triton® x-100 (IB-T, PBS containing 1% v/v goat serum and 0.2% v/v Triton® x-100) at 4°C overnight then rinsed for 2 × 10 min with PBS containing Triton® x-100 (PBS-T, PBS with 0.2% v/v Triton® x-100). Cell nuclei were stained with Hoechst 33258 for 10 min, then rinsed again in PBS.

Images of cells were acquired on a Discovery-1™ automated fluorescence microscope (Molecular Devices, Sunnyvale, CA, USA), fitted with a monochrome peltier cooled 12-bit Hamamatsu CCD camera, using a 40× plan fluorite objective lens (air, NA 0.6) at room temperature with MetaMorph™ software (v6.2r6) (Molecular Devices). Images were acquired using the DAPI (403Ex/465Em), FITC (470Ex/535Em) and TRED (560Ex/650Em) filter sets. Pseudocolouring and merging of images was performed using ImageJ v1.34s (Rasband, 1997–2009).

Confocal imaging

For confocal imaging of the subcellular distribution of huntingtin EGFP, cells were plated at 300 000 cells·well^{-1} onto poly-L-lysine-coated coverslips (#1.5 thickness) in 24-well plates and induced the next day with 1 μM TFZ in full-serum media. After 51 h incubation at 37°C, media was removed and cells fixed with 4% paraformaldehyde for 10 min. Cells were rinsed for 2 × 10 min with PBS, nuclei were stained with Hoechst 33258, 1:500 for 10 min in the dark, and cells were rinsed for a final 2 × 10 min in PBS. Coverslips were mounted with CFPVOH/AF100 antifadant (CitiFluor, Leicester, UK) by inversion onto glass slides. Images were acquired using Leica Scanware 4.2a and equivalent voltage, on a Leica TCS 4D confocal laser scanning microscope (Leica, Wetzlar, Germany) using a 63× plan apochromat objective lens (oil, NA 1.4) at room temperature.

Cannabinoids and drugs

HU210, WIN55212-2, BAY59-3074 and SR141716A were purchased from Tocris Bioscience (Bristol, UK). Due to their hydrophobicity, cannabinoids tend to adsorb to surfaces in the absence of a carrier molecule. All dilutions of cannabinoid drugs were therefore performed in plasticware silanized using Coatasil™ (dimethyl dichlorosilane, Ajax Finechem Ltd., Auckland, New Zealand) as per manufacturer's instructions. The host of carrier proteins in cell culture media animal sera might similarly adsorb cannabinoid ligand, therefore cannabinoid delivery was performed in SFM with 5 mg·mL^{-1} BSA (SFM/BSA) as described by Hillard *et al*. (1995). While absolute cell number was lower under serum-free conditions, relative huntingtin toxicity was indistinguishable from that seen in full-serum conditions. All other drugs were purchased from Sigma (St. Louis, MO, USA) unless otherwise indicated.

Cell survival assays

For survival assays, cells were plated at 35 000 well^{-1} in the central 60 wells of poly-L-lysine (0.2 mg·mL^{-1})-coated 96-well plates. The following day, cells were induced to express huntingtin in the presence of vehicle, cannabinoids, dopaminergics or cAMP modulators. Briefly, media was replaced with SFM/BSA and 0–1 μM TFZ inducer (each with final 0.01% ethanol) with various co-treatments (or their vehicles). These included cannabinoid agonists HU210, WIN55212-2, BAY59-3074 or inverse agonist SR141716A at 0–1 μM, each with final 0.01% ethanol; cAMP-PKA (protein kinase A) binding inhibitor Rp-cAMPS at 100 μM; or the cAMP stimulator forskolin at 10 μM. Due to their superior hydrophilicity, experiments with dopamine (10 μM), D1 antagonist SCH23390 (10 μM), D1 agonist SKF33893 (0–10 μM) and D2 agonist quinpirole (0–10 μM) were performed in full-serum media.

After 72 h, cell viability was assayed by replacing media with SFM/BSA (or full-serum media for dopamine experiments) and the redox indicator Alamar Blue (AbD SeroTec Ltd., Oxford, UK) at 10% (v/v), and returning to incubator for a further 4 h. The fluorescence generated by conversion of Alamar Blue by viable cells was measured at 37°C (Ex/Em 560/590 nm) on a FLUOstar Optima fluorescence plate reader (BMG Labtechnologies, Durham, NC, USA). Percentage cell number was calculated by normalising test cell fluorescence against control cell fluorescence (100%) and fluorescence of Alamar Blue assay solution alone (0%). Depending upon the assay, control cells were represented by cells treated with

either vehicle (0.01% ethanol) or the chosen concentration of test compound (cannabinoid, cAMP modulator or dopaminergic) for the duration of the experiment but *not induced* with TFZ. This allowed specific quantification of drug effect on huntingtin cell death independent of any basal proliferative/toxic effects of the test drug. Figures depict cell death across the TFZ concentration range or at 1 μM TFZ only where the effect was most pronounced at this concentration.

Quantifying the percentage of cells that expressed huntingtin and formed aggregates

After Alamar Blue readings were taken, cells were fixed in 4% paraformaldehyde and then washed in PBS. Cell nuclei were stained with Hoechst 33258 for 10 min, then cells were washed twice in PBS, and imaged at 10× magnification on the Discovery-1™ automated fluorescence microscope. The images were analysed using the Cell Scoring application within MetaMorph™ image analysis software as described previously (Scotter *et al*., 2008).

This application was used to determine either the proportion of cells that expressed detectable levels of huntingtin, or the proportion of cells that contained at least one mutant huntingtin aggregate. This was achieved by quantifying the percentage of Hoechst-positive cells that also had staining in the EGFP wavelength meeting size and intensity criteria for either total huntingtin, or aggregates, as determined from three sample images. For total huntingtin, the criteria were: staining of cytoplasm size, above the intensity of un-induced cells. For aggregates, the criteria were: staining of 1–3 μm, above the maximal intensity achieved by all aggregates in the sample images. We have previously confirmed (Scotter *et al*., 2008) by filter retardation assay that aggregates formed by PC12 97Q cells are characteristic 'insoluble, detergent-resistant' aggregates as seen in other HD models and in human brain (Kazantsev *et al*., 1999; Hoffner *et al*., 2005). Figures depict aggregate formation across the TFZ concentration range, or at 1 μM TFZ only where the effect was most pronounced at this concentration.

cAMP accumulation/PKA binding assay

The cellular accumulation of cAMP was assayed by scintillation counting of tritiated cAMP as described previously (Kearn *et al*., 2005), with the following modifications: cells were plated at 25 000 cells·well^{-1} the day before assay. For G-protein toxin experiments, 4 h after plating, media was replaced with fresh full-serum media containing *Pertussis* toxin (PTX) at 100 ng·mL^{-1} (or 0.05% v/v vehicle: 50% glycerol, 50 mM Tris, 10 mM glycine, 0.5 M NaCl, pH 7.5), and cells were incubated overnight for 18 h. For all assays, on the day of the assay, basal receptor signalling was reduced by 'serum starvation'; cells were incubated with SFM/BSA containing 500 μM 3-isobutyl-1-methyl xanthine (phosphodiesterase inhibitor) for 30 min at 37°C. For assay of the stimulation of cAMP by forskolin, forskolin was added to serum starvation media at 2× concentration in the same media to give 0–250 μM final. For assay of the modulation of cAMP by HU210, HU210 was added to serum starvation media at 2× concentration in the same media to give 0–1 μM final. For assay of the inhibition of cAMP-PKA binding, a cell-free modification of this assay was performed where cell lysate was substituted for 25 μL Rp-cAMPS at 0–100 μM in cAMP assay buffer.

Western blotting

Western blotting for phosphorylated ERK was performed as described previously (Graham *et al*., 2006), with the following modifications: cells were plated at 300 000 cells per well in 24-well plates and were stimulated the next day to mimic conditions in cell survival assays. Plating media was aspirated and cells were stimulated with 1 μM TFZ in SFM/BSA with either vehicle (0.01% ethanol), 1 μM HU210, or 1 μM SR141716A. For $G_{i/o}$ blockade experiments, cells were pretreated for 18 h in full-serum media with PTX at 100 ng·mL^{-1} (or 0.05% v/v vehicle). For ERK blockade experiments, cells were pretreated for 45 min in full-serum media with UO126 at 10 μM (or 0.01% v/v DMSO vehicle).

After appropriate incubation time at 37°C, plates were placed on ice and harvested in 100 μL 1× laemmli buffer (62.5 mM Tris-HCl, pH 6.8, 2% SDS, 10% glycerol) (Laemmli, 1970) and then denatured at 95°C for 5 min. Protein concentration was determined using the Bio-Rad DC Protein Assay, and samples were stored at –85°C until required. Samples were diluted to 0.8 μg·μL^{-1} including final 5% β-mercaptoethanol, and 10 μL of each sample was separated on 10% SDS-polyacrylamide gel at 70 V for 4 h. Proteins were transferred as described previously. Blots were then blocked for 30 min in TBS-T (10 mM Tris Base, 150 mM NaCl, 0.05% Tween 20) containing 1% BSA and then probed overnight at 4°C for pERK (1:1000; catalogue number 9101; Cell Signaling Technology, Beverly, MA, USA), or total ERK (1:2000; catalogue number 9102; Cell Signaling Technology) in TBS-T containing 0.2% BSA. Secondary antibody and ECL detection were performed as described previously, with film exposure times ranging from 20 s to 1 min. Films were scanned using a HP Scanjet 3770 scanner (Hewlett-Packard Co., Palo Alto, CA, USA) at 600 dpi resolution in true colour. Optical density (OD) for pERK was determined by measuring the area under the intensity curve for pERK, as plotted using Gel Analyze in ImageJ, and dividing by the area under the intensity curve for total ERK for that lane. Relative OD was calculated by normalising to the average OD for the vehicle-treated samples.

Immunocytochemistry

For immunocytochemistry for phosphorylated ERK, cells were plated at 100 000 cells·well^{-1} onto poly-L-lysine-coated eight-well culture slides (BD Biosciences, Franklin Lakes, NJ, USA) and were stimulated the next day to mimic conditions in cell death assays. Plating media was aspirated, and cells were stimulated with 1 μM TFZ in SFM/BSA with vehicle (0.01% ethanol), or 1 μM HU210 for 5 min. After appropriate incubation time at 37°C, slides were placed on ice for 2 min during media removal, removed from ice then fixed with 4% paraformaldehyde for 10 min. Cells were rinsed for 2 × 10 min with PBS-T. Epitope unmasking was performed by adding 100 μL·well^{-1} ice-cold methanol (90% v/v) and cooling at –20°C for 10 min. Cells were rinsed for a further 2 × 10 min

in PBS-T then incubated overnight with a distinct α-pERK antibody from that used on Western blots, which was compatible with immunocytochemistry (1:200 in IB-T, catalogue # 4370, raised in rabbit, Cell Signaling Technology). No primary antibody control wells were incubated with IB-T only. Cells were rinsed for 3 × 10 min in PBS-T, then incubated with goat α-rabbit Alexa 488 secondary (1:500 in IB-T, Molecular Probes, Eugene, OR, USA) for 3 h at room temperature. Cells were rinsed for a further 3 × 10 min in PBS-T, then nuclei were stained with Hoechst 33258, 1:500, for 10 min in the dark, before a final 3 × 10 min rinse in PBS-T. The glass slides were mounted with CFPVOH/AF100 antifadant and coverslipped (#1.5 thickness). Images were acquired using a 60× plan fluorite objective lens (air, NA 0.7) at room temperature with NIS-Elements BR software (v3.0) on an Eclipse Ti microscope fitted with a Nikon Coolpix 4500 camera (all Nikon, Melville, NY, USA). Equivalent exposure times for a particular wavelength were used for each drug treatment. Images were merged using Image J 1.34s (http://rsb.info.nih.gov/ij/, NIH, Bethesda, MD, USA).

Statistical analyses

Representative individual experiments are presented in several figures as stated. All other figures or descriptions in the text are the mean ± SEM for pooled data from all repeats. Statistical analyses were performed on pooled data (for each cell type individually) by one-way repeated measures ANOVA with Bonferroni multiple comparison post testing using GraphPad Prism® 4.02 (GraphPad Software Inc., La Jolla, CA, USA).

Results

PC12 cells endogenously expressed D2 dopamine but not D1 dopamine or CB_1 cannabinoid receptors

PCR was carried out to examine expression of endogenous dopamine or cannabinoid receptors in PC12 cells. PC12 cells transfected with 25Q or 97Q huntingtin constructs were found to endogenously express the D2 dopamine receptor, at low levels compared with brain, but not the D1 dopamine receptor or the CB_1 cannabinoid receptor (Figure 1). The absence of endogenous CB_1 is consistent with our findings by RT-PCR and binding assay (data not shown), and those of Aiken *et al*. by immunoblot (Aiken *et al*., 2004), in the parental PC12 cells. Drug effects on cell lines not transfected with the target receptor could therefore be considered to be independent of activity at these receptors. Whole cell binding assays showed specific binding equivalent to 25.2 ± 4.4 fmol·mg^{-1} in PC12 97Q CB1 cells and 22.7 ± 1.2 fmol·mg^{-1} in PC12 25Q CB1 cells. No specific binding was detected in untransfected PC12 cells (data not shown).

Huntingtin cell death was time- and inducer concentration-dependent

Induction of PC12 25Q cells with TFZ leads to diffuse expression of EGFP-tagged huntingtin, throughout the cytoplasm and, to a lesser degree, also the nucleus (Figure 2A). Induction

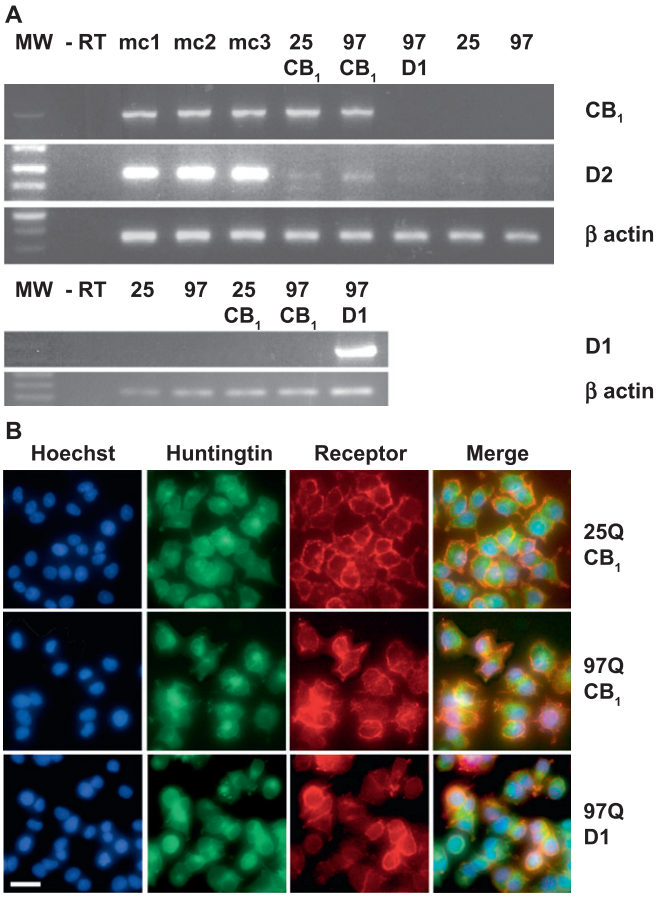

Figure 1 (A) RT-PCR analysis of G-protein-coupled receptors expressed by PC12 cells showed that there was a low level of endogenous expression of the D2 dopamine receptor, but no detectable D1 dopamine receptor or CB_1 cannabinoid receptor, unless transfected (–RT, no reverse transcriptase, mc, mouse cerebellum-positive control). (B) Photomicrographs captured by Discovery-1 of PC12 25Q and 97Q cells induced with 1 μM tebufenozide for 24 h, 'live-labelled' with mouse α-HA.11 primary antibody, then labelled post fixation with Alexa 594 α-mouse secondary antibody confirmed that both HA-tagged CB1 and D1 receptors were localized to the cell surface. One representative image shown for each cell type, 40× objective, scale bar = 20 μm.

of PC12 97Q cells leads to a similar initial distribution of EGFP-tagged huntingtin; however, diffuse huntingtin formed intensely fluorescent aggregates in an increasing number of cells over time. The majority of aggregate-positive cells contained one large cytoplasmic aggregate; however, there were also instances of more than one large cytoplasmic aggregate or numerous small nuclear/perinuclear aggregates (Figure 2B).

The proportion of cells that expressed detectable levels of huntingtin was well correlated to the concentration of TFZ in this tightly regulated expression system (Figure 2C and D). PC12 cells showed significant and extensive reductions in Alamar Blue conversion in response to huntingtin expression, in a manner that was time-dependent and concentration-dependent with respect to the TFZ inducer (Figure 2E and F). The redox indicator Alamar Blue is converted in live cells by various mitochondrial and cytoplasmic enzymes (Gonzalez and Tarloff, 2001) to give a measure of the number of living cells, rather than a measure of their viability. We found an

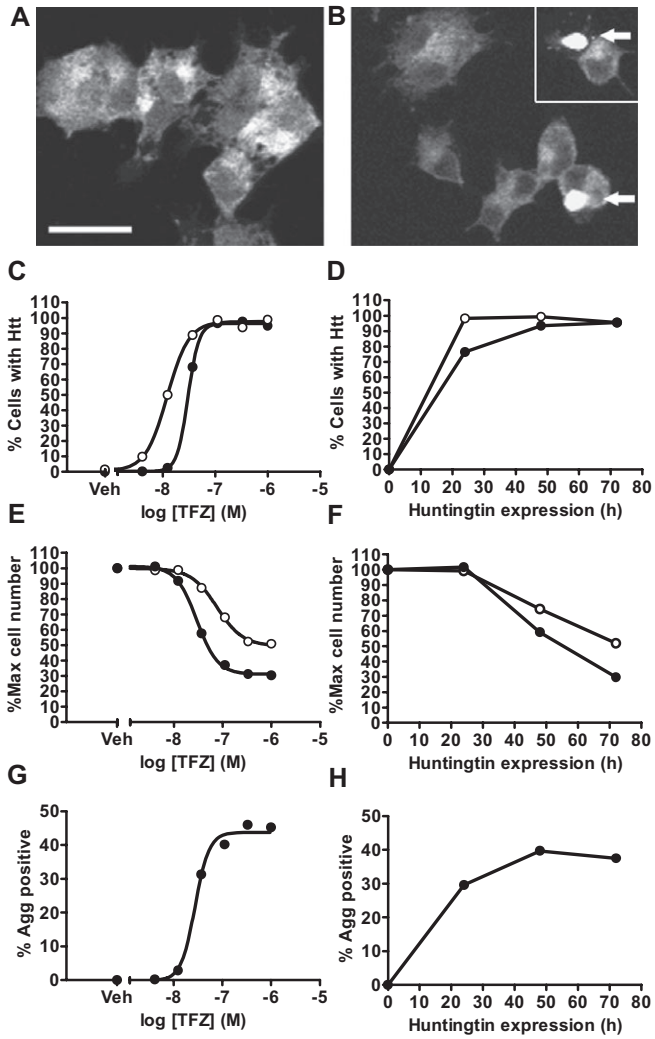

Figure 2 Confocal photomicrographs of (A) PC12 25Q cells and (B) PC12 97Q cells, each induced with 1 μM tebufenozide (TFZ) for 48 h. 25Q huntingtin showed diffuse, predominantly cytoplasmic expression. 97Q huntingtin was also predominantly diffuse in the cytoplasm however some cells formed large aggregates of 97Q protein in the cytoplasm (arrows inc. inset) or occasionally smaller aggregates in the nucleus (not shown). One representative image shown for each cell type, scale bar = 20 μm. (C) Percentage of PC12 cells that are positive for huntingtin after 72 h induction with 0–1 μM TFZ (n = 1). (D) Percentage of PC12 cells that are positive for huntingtin after induction with 1 μM TFZ for 0–72 h (n = 1). (E) Percentage of PC12 cells remaining after 72 h induction with 0–1 μM TFZ [significant death: 25Q = $F(6,98)$ = 155.6, 111 nM–1 μM TFZ, $P < 0.001$; 97Q = $F(6,97)$ = 276.4, 37 nM–1 μM TFZ, $P < 0.001$]. (F) Percentage of PC12 cells remaining after induction with 1 μM TFZ for 0–72 h [significant death: 25Q = $F(3,56)$ = 348.9, 48–72 h, $P < 0.001$; 97Q = $F(3,56)$ = 291.6, 48–72 h, $P < 0.001$]. (G) Percentage of PC12 97Q cells that are positive for 97Q huntingtin aggregates (Agg) following 72 h induction with 0–1 μM TFZ (n = 2). (H) Percentage of PC12 97Q cells that are positive for 97Q huntingtin aggregates following induction with 1 μM TFZ for 0–72 h (n = 2). Representative experiment shown for each cell type, n = 3 unless stated otherwise. Symbols: ○ PC12 25Q; ● PC12 97Q.

excellent correlation, across a range of cell viabilities, between Alamar Blue fluorescence and cell counts measured using a Discovery-1™ automated fluorescence microscope and MetaMorph™ image analysis software (data not shown). Alamar Blue was therefore used as an indirect assay for cell number. Lactate dehydrogenase assays confirmed that this TFZ concentration-dependent decrease in cell number was due to cell death rather than an inhibition of proliferation (data not shown).

Interestingly, expression of *either* 25Q or 97Q exon one huntingtin protein was toxic to PC12 cells, although both the potency and extent of the death response was greater with 97Q Htt expression (Figure 2E, 25Q: EC_{50} = 167.5 ± 47.1 nM, cells remaining with 1 μM TFZ = 56.7 ± 1.6%; 97Q: EC_{50} = 34.0 ± 6.0 nM, cells remaining with 1 μM TFZ = 34.1 ± 1.7%). Hereafter 25Q huntingtin is therefore referred to as 'wildtype' to acknowledge that it differs from full-length wild-type huntingtin.

The aggregate formation seen in PC12 97Q cells was dependent upon both the concentration of mutant huntingtin protein, with an EC_{50} of 30.3 ± 2.7 nM TFZ, and the expression time (Figure 2G and H), consistent with previous reports of amyloid-like, nucleation-dependent aggregation of mutant huntingtin (Scherzinger *et al*., 1999; Chen *et al*., 2001).

Huntingtin cell death is modulated by cellular cAMP levels

Cell death due to mutant huntingtin expression was alleviated by the cannabinoid agonists HU210 and WIN55212-2 and exacerbated by the inverse agonist SR141716A. As shown in Figure 1, PC12 cells did not endogenously express the CB_1 cannabinoid receptor. Accordingly, CB_1-negative PC12 cells (PC12 25Q/97Q) showed no significant change in the cell death due to expression of 'wildtype' or mutant exon one Htt when co-treated with the classical cannabinoid agonist HU210 or inverse agonist SR141716A (Figure 3A and C). In PC12 cells transfected with human CB_1 receptor and expressing 'wildtype' exon one Htt (PC12 25Q CB_1), neither ligand significantly altered the cell death profile (Figure 3B). In contrast, in CB_1-transfected cells expressing *mutant* exon one Htt (PC12 97Q CB_1), HU210 co-treatment caused a small but significant and reproducible reduction in the extent of cell death (Figure 3D, 7.9 ± 2.0% reduction). This alleviation of mutant huntingtin cell death by HU210 was concentration-dependent, with maximal rescue of death seen with 1 μM HU210 (Figure 3E). In accordance with this, the inverse agonist SR141716A caused a small exacerbation of cell death in PC12 97Q CB_1 cells treated with 1 μM TFZ (Figure 3D and F, 3.3 ± 1.3% exacerbation).

Two other cannabinoid agonists, the synthetic full agonist WIN55212-2 and the synthetic low-efficacy agonist BAY59-3074, were also investigated as potential cell death modifiers. When applied at 1 μM, there was no effect of either WIN55212-2 or BAY59-3074 on PC12 25Q or PC12 25Q CB_1 cells (Figure 4A and B). However, both compounds showed a small degree of protection in PC12 97Q CB_1 cells induced with 1 μM TFZ (Figure 4D, WIN: 6.4 ± 1.1%, BAY: 4.4 ± 1.7%). Interestingly, BAY59-3074 co-treatment improved HD cell survival similarly in CB_1-*negative* PC12 97Q cells, indicating a receptor-independent mechanism (Figure 4C, 3.1 ± 1.3%). Indeed, while the alleviation of mutant huntingtin cell death in PC12 97Q CB_1 cells by WIN55212-2 was concentration-dependent, BAY59-3074 conferred protection only at the 1 μM concentration, far higher than its reported K_i

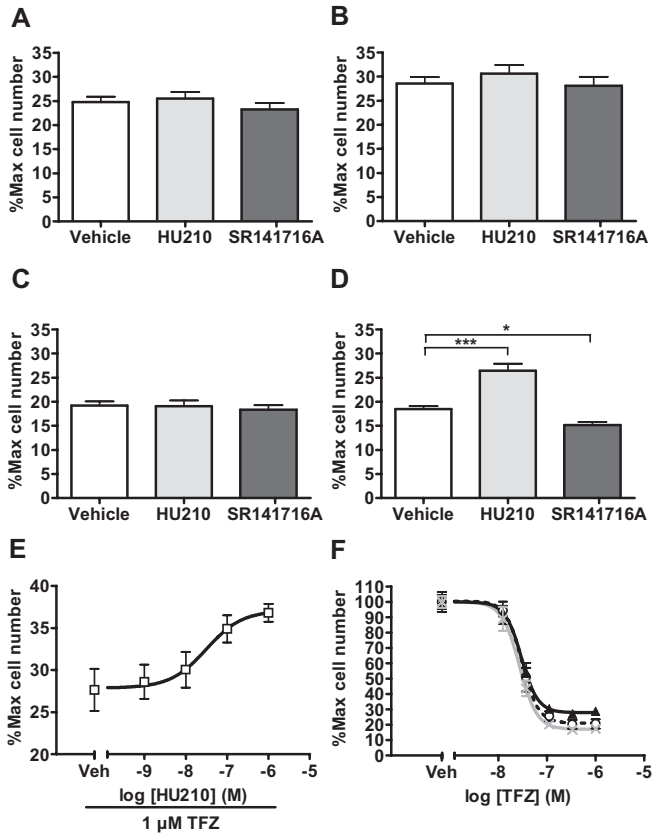

Figure 3 Huntingtin-induced death at 72 h in CB_1-negative PC12 cells expressing (A) 25Q or (C) 97Q exon one huntingtin, or in CB_1-transfected cells expressing (B) 25Q or (D) 97Q exon one huntingtin, due to induction with 1 μM tebufenozide (TFZ) and co-treatment with vehicle (Veh) (0.01% EtOH), HU210 (1 μM) or SR141716A (1 μM). There was a significant reduction of 97Q huntingtin-induced death by HU210 [$F(2,37) = 34.81$, 7.9 ± 2.0%, $P < 0.001$], and exacerbation of death by SR141716A [$F(2,37) = 34.81$, 3.3 ± 1.3%, $P < 0.05$] in CB_1-transfected cells. (E) This reduction of cell death by HU210 was concentration-dependent with maximal rescue seen at 1 μM HU210. (F) Huntingtin-induced death at 72 h in PC12 97Q CB_1 cells due to induction with 0–1 μM TFZ and co-treatment with (-○-) vehicle (0.01% EtOH) (▲) HU210 (1 μM) or (×) SR141716A (1 μM). (A–D) were derived from TFZ concentration range experiments such as this, which show that the maximal effect of HU210 occurred at 1 μM TFZ. Pooled data shown for (A–D), representative experiment shown for (E and F), mean ± SEM, $n = 4$. *, $P < 0.05$; ***, $P < 0.001$.

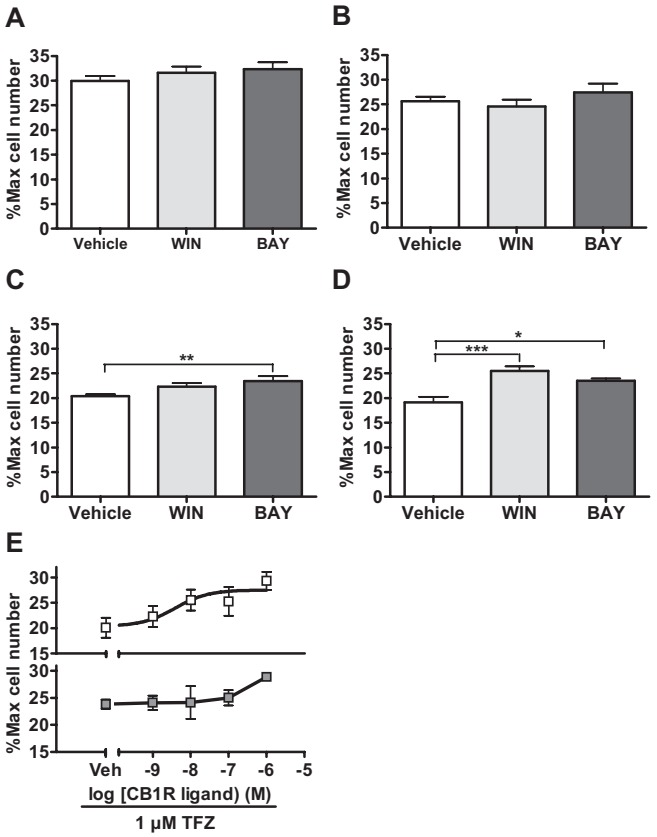

Figure 4 Huntingtin-induced death at 72 h in CB_1-negative PC12 cells expressing (A) 25Q or (C) 97Q exon one huntingtin, or in CB_1-transfected cells expressing (B) 25Q or (D) 97Q exon one huntingtin, due to induction with 1 μM tebufenozide and co-treatment with vehicle (Veh) (0.01% EtOH), WIN55212-2 (1 μM) or BAY59-3074 (1 μM). There was a significant modulation of 97Q huntingtin-induced cell death in CB_1-transfected but not CB_1-negative cells by WIN55212-2 [6.4 ± 1.1%, $F(2,17) = 11.73$, $P < 0.001$]. BAY59-3074 shows CB_1 receptor-independent rescue, modifying 97Q huntingtin-induced cell death in both CB_1-negative and CB_1-transfected cells [PC12 97Q: $F(2,17) = 5.783$, 3.1 ± 1.3%, $P < 0.01$; PC12 97Q CB_1: $F(2,17) = 11.73$, 4.4 ± 1.7%, $P < 0.05$]. (E) Consistent with a CB_1-dependent mechanism, reduction of cell death by WIN55212-2 (□) showed ligand concentration dependence. BAY59-3074 (■) reduced cell death only at 1 μM. Pooled data shown for (A–D), representative experiment shown for (E), mean ± SEM, $n = 3$. *, $P < 0.05$; **, $P < 0.01$; ***, $P < 0.001$.

at the human CB_1 receptor, of 48.3 nM (De Vry *et al*., 2004) (Figure 4E).

Cell death due to huntingtin expression was exacerbated by forskolin but unchanged by Rp-cAMPS. We examined the potential involvement of cyclic adenosine monophosphate (cAMP) modulation in HU210-mediated protection against mutant huntingtin toxicity. We first validated the ability of the adenylate cyclase activator forskolin to increase cAMP levels, and the ability of Rp-cAMPS to inhibit binding of cAMP to PKA. We found that treatment of cells with 28–250 μM forskolin significantly increased intracellular cAMP concentration (Figure 5A). In a cell-free modification of the same assay, Rp-cAMPS inhibited the binding of [^{3}H]-cAMP to PKA significantly at 100 μM, however only weakly and not at lesser concentrations (Figure 5B, 17.2% inhibition). In cell survival assays, cAMP stimulation by 10 μM forskolin significantly exacerbated cell death due to expression of either 'wildtype' or mutant huntingtin (Figure 5C and D, PC12 25Q: 15.0 ± 3.0% increase; PC12 97Q: 9.2 ± 3.2% increase). Rp-cAMPS did not significantly modify cell death due to expression of either 'wildtype' or mutant huntingtin; however, this may have been due to its poor efficacy in inhibiting cAMP binding to PKA. Together with the cannabinoid findings, these data suggested that the modulation of cAMP levels may influence cell survival in huntingtin-expressing cells.

Cell death due to huntingtin expression was exacerbated by D1 dopaminergic signalling. To further test this hypothesis, we employed D1 dopamine receptor stimulation to investigate the effect of G_s signalling. PC12 cells endogenously expressed the D2 but not D1 subtype, as assessed by RT-PCR (Figure 1).

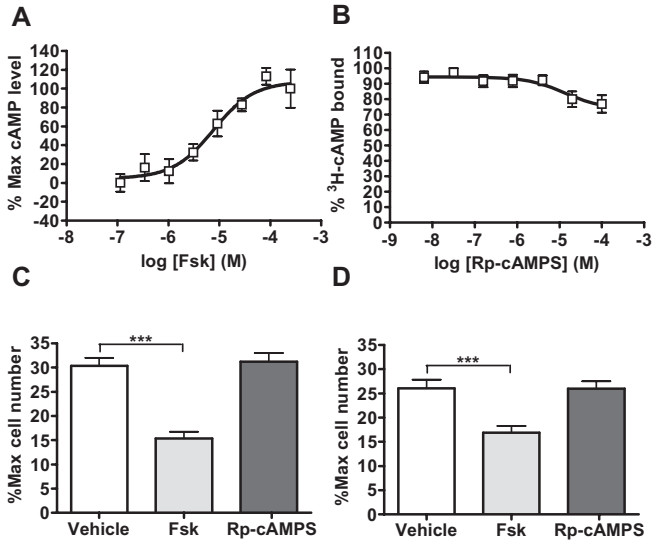

Figure 5 (A) Accumulation of cAMP in un-induced (no TFZ) PC12 cells stimulated with forskolin [$F(9,96) = 11.26$, 28–250 μM Fsk all $P < 0.001$, $n = 2$] and (B) inhibition of [^{3}H]-cAMP binding to protein kinase A in the presence of Rp-cAMPs (100 μM: 17.2%, $n = 1$). Huntingtin-induced death at 72 h in PC12 cells expressing (C) 25Q or (D) 97Q exon one huntingtin, due to induction with 1 μM TFZ and co-treatment with vehicle (0.02% DMSO), forskolin (10 μM) or Rp-cAMPS (100 μM). There was a significant exacerbation of both 25Q and 97Q huntingtin-induced toxicity by forskolin [25Q: $F(2,45) = 29.7$, 15.0 ± 3.0% exacerbation, $n = 5$; 97Q: $F(2,36) = 9.75$, 9.2 ± 3.2% exacerbation, $n = 4$; both $P < 0.001$]. There was no significant change in huntingtin-induced toxicity with Rp-cAMPS co-treatment. Representative experiments shown for (A and B), pooled data shown for (C and D), mean ± SEM, $n = 3$. ***, $P < 0.001$.

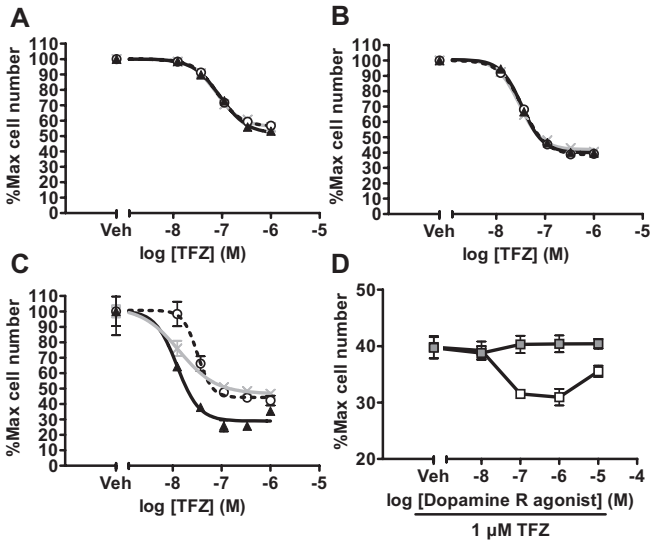

Figure 6 Huntingtin-induced death at 72 h in D1-negative PC12 cells expressing (A) 25Q or (B) 97Q exon one huntingtin, or in D1-transfected cells expressing (C) 97Q exon one huntingtin, due to induction with 0–1 μM tebufenozide (TFZ) and co-treatment with (-○-) vehicle (0.1% EtOH) (▲) dopamine (10 μM) or (×) SCH23390 (10 μM). Pooling of data from independent experiments showed a significant exacerbation of 97Q huntingtin-induced cell death with 333 nM TFZ for dopamine [$F(2,25) = 19.93$, 16.7 ± 5.8%, $P < 0.001$] but not SCH23390 in D1-transfected cells. (D) Consistent with a D1-dependent mechanism, the D1 agonist (□) SKF38393, but not the D2 agonist (■) quinpirole, showed exacerbation of cell death when applied at 100 nM–1 μM in PC12 97Q D1 cells at 72 h [$F(4,34) = 8.047$, $P < 0.01$]. Representative experiment shown for each cell type, mean ± SEM, $n = 3$.

Exogenous dopamine had no significant effect on the viability of D1-negative PC12 cells expressing wild-type or mutant exon one Htt (Figure 6A and B). However, in PC12 cells transfected with human D1 (PC12 97Q D1), exogenous dopamine significantly exacerbated the cell death due to expression of mutant Htt expression at concentrations from 12–333 nM TFZ (Figure 6C). Surprisingly, at low TFZ concentrations, the D1-specific antagonist SCH23390 also significantly exacerbated the extent of cell death in PC12 97Q D1 cells. SCH23390 did not significantly alter the profile of cell death in D1-negative PC12 97Q cells, indicating that the D1 was required for this effect (Figure 6C).

To further confirm that the detrimental effect of dopamine was D1-mediated, the selective D1 or D2 agonists, SKF38393 and quinpirole, respectively, were tested for their ability to modify mutant huntingtin-induced cell death. Figure 6D shows that in PC12 97Q D1 cells induced with 1 μM TFZ for 72 h, SKF38393, but not quinpirole, mimics dopamine potentiation of huntingtin toxicity. Co-treatment with 1 μM SKF38393 reduced cell number by 8.5 ± 2.6% compared with vehicle co-treatment, whereas 1 μM quinpirole co-treatment did not significantly alter cell death. These data support a detrimental effect of D1 signalling in mutant huntingtin-expressing cells.

HU210-mediated rescue of huntingtin cell death is dependent upon $G_{i/o}$ and ERK

Functional $G_{i/o}$ was required for HU210-mediated rescue of huntingtin cell death. Results so far indicated that various compounds that elevate cAMP levels exacerbated huntingtin-mediated cell death, and cannabinoid compounds, which decrease cAMP levels (Howlett *et al*., 1986), alleviated huntingtin-mediated cell death. We therefore tested whether HU210-mediated rescue of huntingtin cell death was in fact dependent upon $G_{i/o}$ coupling, which links CB_1 to the inhibition of cAMP. PTX ablation of $G_{i/o}$ was confirmed by cAMP assay, which showed a blockade of the cAMP inhibition caused by HU210, and a switch to G_s coupling, as described previously (Glass and Felder, 1997; Bonhaus *et al*., 1998) (Figure 7A). It has not been determined whether it is the $G_{i/o}$ subunits or the βγ they release that are responsible for adenylate cyclase inhibition, therefore the term '$G_{i/o}$' is used to encompass all possible effectors. The EC_{50} values for inhibition or stimulation of cAMP by HU210 were 0.26 ± 0.10 nM and 24.7 ± 14.5 nM, respectively, indicating that at the 1 μM HU210 concentration predominantly used in this study, the CB_1 receptor is capable of activating either $G_{i/o}$ or G_s.

In PC12 97Q CB_1 cells subjected to this PTX ablation before huntingtin expression and HU210 treatment were initiated, the concentration-dependent alleviation of huntingtin cell death by HU210 was abolished [Figure 7B, vehicle (veh) pretreat: 5.8 ± 1.7% rescue by HU210; PTX pretreat: 0.4 ± 1% rescue by HU210]. Functional $G_{i/o}$ was therefore required for HU210-mediated rescue of huntingtin cell death. In addition, the extent of huntingtin cell death induced by 1 μM TFZ alone (without HU210 co-treatment) was exacerbated by PTX pretreatment (Figure 7B, veh pretreat: 32.5 ± 1.0% cells

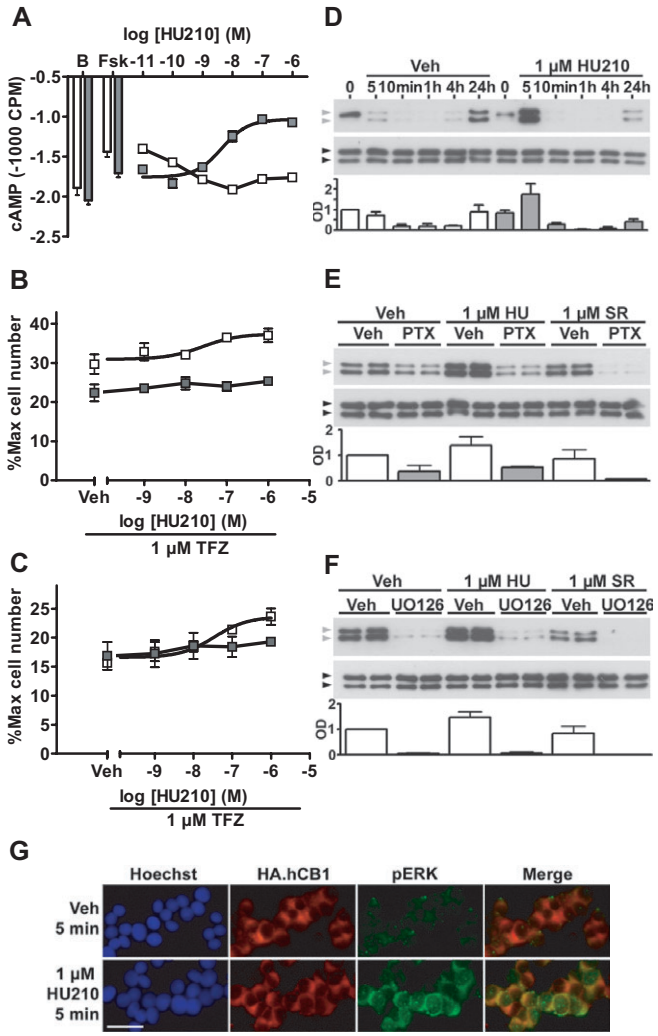

Figure 7 (A) HU210-mediated changes in cAMP accumulation in PC12 97Q CB_1 cells pretreated with (□) vehicle or (■) *Pertussis* toxin (PTX, 100 ng·mL^{-1}, 18 h) relative to basal (B) or forskolin (Fsk)-induced cAMP levels. While the CB_1 was coupled primarily to the inhibition of cAMP, $G_{i/o}$ ablation by PTX unveiled the stimulatory potential of CB_1 on cAMP. (B) Huntingtin-induced death at 72 h in PC12 97Q CB_1 cells pretreated with (□) vehicle or (■) PTX (100 ng·mL^{-1}, 18 h) then induced with 1 μM TFZ with co-application of various concentrations of HU210 [$F(3,52) = 90.03$, veh pretreat: 5.8 ± 1.7% rescue by HU210, $P < 0.001$; PTX pretreat: 0.4 ± 1% rescue by HU210, ns]. (C) Huntingtin-induced death at 72 h in PC12 97Q CB_1 cells pretreated with (□) vehicle or (■) UO126 (10 μM, 45 min) then induced with 1 μM TFZ with co-application of various concentrations of HU210 [$F(3,39) = 4.65$, veh pretreat: 7.1 ± 2.4% rescue by HU210, $P < 0.01$; UO126 pretreat: 0.8 ± 3% rescue by HU210, ns]. One representative experiment shown for each cell type, mean ± SEM, $n = 3$, statistics shown are for pooled data. (D–F) Western blots of (►) pERK and (▻) total ERK to show (D) the time course of HU210-mediated ERK phosphorylation; and blockade of HU210-mediated ERK phosphorylation by (E) PTX pretreatment or (F) UO126 pretreatment. One representative experiment shown for each cell type, mean ± SEM, Optical density (OD) of pERK/total ERK, relative to vehicle control, for pooled data, $n = 2$. These data show that HU210 conferred rescue against huntingtin-induced cell death in a concentration-dependent manner, unless pretreated with PTX or UO126. This may correlate with the ability of PTX or UO126 pretreatment to block HU210-induced phosphorylation of ERK. (G) Photomicrograph of PC12 97Q CB_1 cells stimulated with vehicle (0.01% EtOH) or 1 μM HU210 for 5 min, and immunolabelled for CB_1 receptors (CB_1) and phosphorylated ERK (pERK). HU210 induced pERK in the majority of cells, suggesting that while pERK was necessary for the HU210 rescue effect, it was not sufficient alone. Scale bar = 20 μm. One image shown for each condition from a representative experiment, $n = 3$.

remain; PTX pretreat: 24.5 ± 0.6% cells remain). This would be consistent with the uncoupling of all tonically active $G_{i/o}$-linked GPCRs with protective signalling capacities, which may comprise various GPCR subtypes, or CB_1 alone. Activation of the D2, which is also $G_{i/o}$-linked, was unable to improve cell survival. While this may be a function of the low level of endogenous D2 expression compared with brain, D2 receptor signalling has previously been shown to potentiate the toxicity of mutant huntingtin (Charvin *et al.*, 2005). The protective effect of cAMP inhibition may therefore be specific to activation by CB_1 or to certain $G_{i/o}$-linked pathways.

ERK phosphorylation was required for HU210-mediated rescue of huntingtin cell death. One CB_1-mediated signalling pathway modulated by cAMP is the activation of ERK. Pretreatment of PC12 97Q CB_1 cells with the MEK1 inhibitor UO126 before induction of huntingtin expression did not change the extent of cell death induced by 1 μM TFZ. However, in these UO126-pretreated cells, HU210 was no longer able to concentration-dependently alleviate huntingtin cell death (Figure 7C, veh pretreat: 7.1 ± 2.4% rescue by HU210; UO126 pretreat: 0.8 ± 3% rescue by HU210). ERK is widely thought to be the sole phosphorylation substrate for MEK1, therefore it can be considered that the phosphorylation of ERK was required for HU210-mediated rescue of huntingtin cell death.

ERK phosphorylation following HU210 treatment is rapid, transient and sensitive to both PTX and UO126. The cellular outcomes following ERK phosphorylation differ greatly depending upon whether ERK stimulation is transient or sustained (Ebisuya *et al.*, 2005). We analysed the time frame of ERK phosphorylation following HU210 (or vehicle) co-treatment in PC12 97Q CB_1 cells, under the same conditions as for cell survival assays, in order to determine the early profile of ERK in relation to the cell survival outcomes already assayed. There was a transient increase in ERK phosphorylation in cells co-treated with 1 μM HU210 (Figure 7D). We predicted that the rescue of huntingtin cell death conferred by HU210 co-treatment was related to this early, transient peak of pERK. We confirmed that the peak in pERK levels at 5 min following HU210 co-treatment was sensitive to both PTX (Figure 7E) and UO126 (Figure 7F). Further supporting a protective role for pERK induction, SR141716A, which exacerbated huntingtin cell death, tended to negatively regulate pERK (Figure 7E and F).

Interestingly, UO126 pretreatment prevented cellular rescue via CB_1, but did not otherwise exacerbate huntingtin-induced cell death. This may be due to the fact that pERK is necessary for protection against huntingtin-induced cell death, but not sufficient. Indeed Figure 7G shows that pERK is significantly elevated following 5 min HU210 treatment, compared with 5 min vehicle treatment, in the majority of

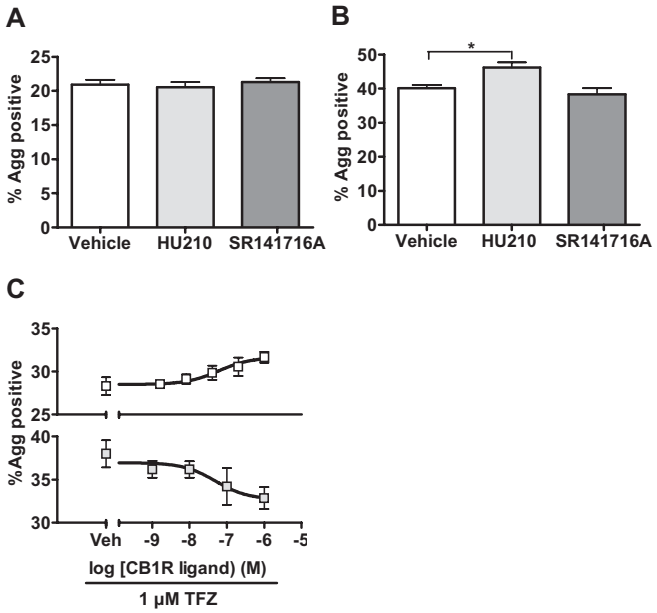

Figure 8 Formation of 97Q huntingtin aggregates (Agg) at 72 h in (A) CB_1-negative or (B) CB_1-transfected PC12 cells expressing 97Q exon one huntingtin, following induction with 1 μM tebufenozide (TFZ) and co-treatment with vehicle (0.01% EtOH), HU210 (1 μM) or SR141716A (1 μM). HU210, but not SR141716A, modulated the proportion of aggregate-positive cells in CB_1-transfected cells [$F(2,25) = 7.018$, 6.1 ± 2.6% increase, $P < 0.05$]. (C) The (□) HU210-mediated increase in aggregate formation at 1 μM TFZ was concentration-dependent with a significant increase from vehicle (Veh) seen at 1 μM HU210. This treatment paradigm also revealed a concentration-dependent inhibitory effect of (■) SR141716A upon aggregate formation. Pooled data shown for (A and B), representative experiment shown for (C), mean ± SEM, $n = 3$. *, $P < 0.05$.

cells. In spite of this increase in pERK in most of the cell population, an increase in survival of less than 10% (7.1 ± 2.4%) was found. This suggests that pERK alone is not sufficient, and that only a small proportion of cells express the additional factors required to transduce the pERK signal into cellular rescue.

Huntingtin aggregate formation

HU210 and activators of the cAMP pathway enhanced huntingtin aggregate formation. We have described a small but highly reproducible, concentration-dependent protective effect for HU210 against mutant huntingtin cell death in PC12 97Q CB_1 cells. Surprisingly, however, HU210 caused an *increase* in the percentage of PC12 97Q CB_1 cells that formed mutant huntingtin aggregates over the 72 h induction period with 1 μM TFZ (Figure 8B, 6.1 ± 2.6% increase). This increase in aggregates was specific to CB_1-transfected cells, indicating a receptor-dependent mechanism, with CB_1-negative PC12 97Q cells showing no change in aggregate formation with HU210 (Figure 8A). Also supporting a CB_1 receptor-dependent pathway, the increase in aggregates by HU210 was concentration-dependent, with maximal aggregate formation seen with 1 μM HU210 (Figure 8C).

There was no significant modulation of aggregate formation by WIN55212-2 or BAY59-3074 in either PC12 97Q or 97Q CB_1 cells (data not shown). While there was also no detectable modulation of aggregate formation by SR141716A in Figure 8A and B, the modified treatment paradigm using a constant concentration (1 μM) of TFZ and increasing concentrations of SR141716A revealed a concentration-dependent inhibitory effect of SR141716A upon aggregate formation in PC12 97Q CB_1 cells, which was in keeping with its activity as an inverse agonist of CB_1 (Figure 8C).

Huntingtin aggregate formation was unchanged by Rp-cAMPS but enhanced by forskolin in PC12 cells. While our findings for HU210 suggested a correlation between cellular rescue and increased aggregate load, the 9.2 ± 1.9% exacerbation of PC12 97Q cell death by forskolin correlated with an almost doubling in the percentage of these cells containing mutant huntingtin aggregates (Figure 9A, 17.9 ± 3.9% increase). There was no reduction in aggregate load seen with Rp-cAMPs. The finding of increased aggregate load associated with forskolin toxicity is surprising in light of the increased aggregate load associated with a beneficial effect of HU210. It appears that either there is a complex relationship between aggregate load and cell number, or that the pathway for modulation of cell survival, via $G_{i/o}$, inhibition of cAMP, and phosphorylation of ERK 1/2, is not involved in the modulation of aggregate formation, and this was investigated further.

Huntingtin aggregate formation was enhanced by D1 dopaminergic signalling in PC12 cells. In D1-negative PC12 97Q cells, neither dopamine nor SCH23390 significantly altered the proportion of cells that developed aggregates of mutant huntingtin after 72 h induction using a range of TFZ concentrations (Figure 9B). Interestingly, in PC12 97Q D1 cells, both dopamine *and* SCH23390 caused a leftward shift in the TFZ concentration–response of aggregate formation and significantly increased the percentage of aggregate-positive cells at all concentrations of TFZ tested (Figure 9C).

Although there was no modulation of aggregate formation by dopaminergics in D1-negative cells, the finding that both dopamine and SCH23390 acted to enhance aggregate formation in D1-transfected cells suggested that further investigation into the dopamine receptor subtype involved was warranted. As described for the exacerbation of huntingtin cell death, the enhancement of aggregates by dopamine also appeared to be specifically D1-mediated. In PC12 97Q D1 cells, the selective D1 agonist, SKF38393, but not the selective D2 agonist, quinpirole, concentration-dependently increased the formation of mutant huntingtin aggregates due to 1 μM TFZ induction (Figure 9D).

HU210-mediated enhancement of aggregate formation proceeds through a different pathway to HU210-mediated alleviation of huntingtin cell death

HU210 was synergistic with forskolin in increasing mutant huntingtin aggregate load. The next indication that the modulation of aggregate load by HU210 may proceed through an alternate pathway to the modulation of cell survival came when investigating synergy between HU210 and forskolin in enhancing the formation of huntingtin aggregates. In PC12 97Q cells there was an enhancement of mutant huntingtin

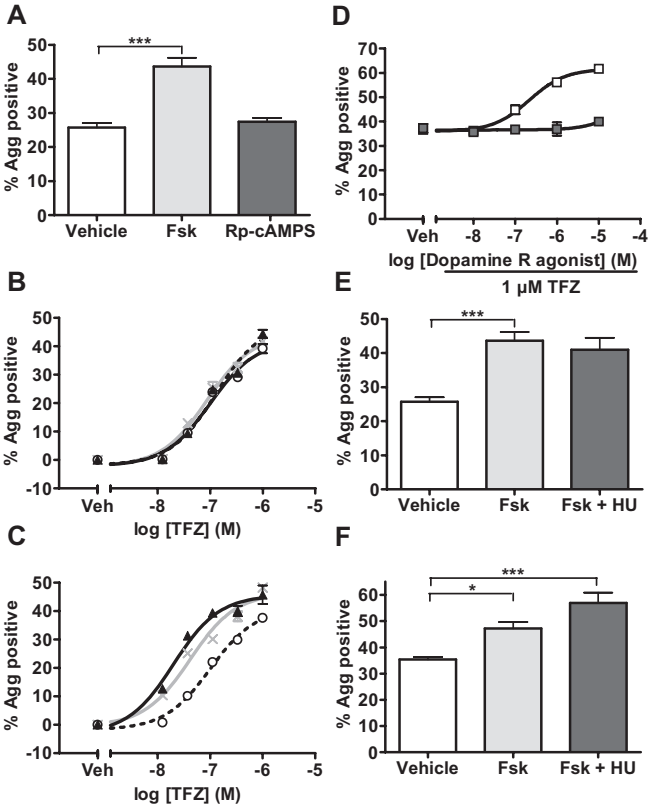

Figure 9 (A) Formation of 97Q huntingtin aggregates (Agg) at 72 h in PC12 97Q cells treated with 1 μM tebufenozide (TFZ) and co-treated with vehicle (Veh) (0.02% DMSO), forskolin (Fsk) (10 μM) or Rp-cAMPS (100 μM). There was a significant increase in the proportion of aggregate-positive cells by forskolin [$F(2,27) = 31.27$, 17.9 ± 3.9%, $P < 0.001$] but no change by Rp-cAMPS. Formation of 97Q huntingtin aggregates at 72 h in (B) D1-negative or (C) D1-transfected PC12 97Q cells treated with (-○-) vehicle (0.1% EtOH) (▲) dopamine (10 μM) or (×) SCH23390 (10 μM). Pooling of data from independent experiments showed a significant increase in the proportion of aggregate-positive cells, at 1 μM TFZ, by dopamine (14.6 ± 4.3%, $P < 0.001$) and SCH23390 (10.6 ± 3.4%, $P < 0.01$) in D1-transfected cells, but no change by either compound in D1-negative cells. (D) Consistent with a D1-dependent mechanism for potentiation of aggregate formation, the D1 agonist (□) SKF38393, but not the D2 agonist (■) quinpirole, increased the proportion of aggregate-positive PC12 97Q D1 cells at 72 h due to 1 μM TFZ induction, in a concentration-dependent manner. Formation of 97Q huntingtin aggregates at 72 h in (E) CB_1-negative or (F) CB_1-transfected PC12 97Q cells treated with 1 μM TFZ and co-treated with vehicle (0.01% DMSO, 0.1% EtOH), forskolin (Fsk, 10 μM) or forskolin + HU210 (10 μM + 1 μM). There was an enhancement of 97Q huntingtin aggregate formation by forskolin in both PC12 97Q and PC12 97Q CB_1 cells [97Q: $F(2,27) = 16.89$, 17.9 ± 3.9%, $P < 0.001$; 97Q CB_1: $F(2,26) = 19.88$, 11.9 ± 3.4%, $P < 0.01$]. In PC12 97Q cells, HU210 did not significantly enhance forskolin-potentiated huntingtin aggregate formation. However, in PC12 97Q CB_1 cells there was synergy between forskolin and HU210 in increasing aggregate load ([Fsk: 11.9 ± 3.4%; HU210: 6.1 ± 2.6% (Figure 8B); Fsk + HU: 21.6 ± 5.0% increase from veh]. Representative experiment shown for each cell type, mean ± SEM, $n = 3$. *, $P < 0.05$; ***, $P < 0.001$.

aggregate formation with 1 μM TFZ when co-treated with forskolin (Figure 9E, 17.9 ± 3.9% increase from veh). The addition of HU210 to the TFZ/forskolin co-treatment in these CB_1-negative cells did not significantly enhance huntingtin aggregate formation above the level of TFZ/forskolin co-treatment.

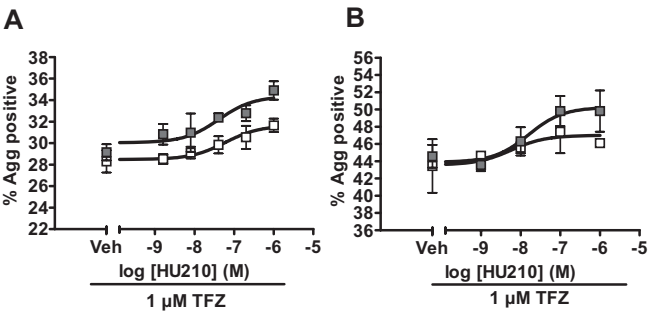

Figure 10 Formation of 97Q huntingtin aggregates (Agg) at 72 h in PC12 97Q CB_1 cells pretreated with (A) (□) vehicle (Veh) or (■) *Pertussis* toxin (PTX, 100 ng·mL^{-1}, 18 h) or (B) (□) vehicle or (■) UO126 (10 μM, 45 min) then induced with 1 μM tebufenozide (TFZ) with co-application of HU210 at increasing concentrations. HU210 increased the proportion of aggregate-positive cells in a concentration-dependent manner, even when pretreated with PTX or UO126. Pooling of data from independent experiments showed a trend towards increased aggregate formation with 1 μM HU210 in vehicle-pretreated cells but this was not statistically significant. This trend was maintained when cells were pretreated with either PTX or UO126 indicating that neither $G_{i/o}$ nor pERK were necessary for the HU210-mediated increase in aggregate formation. Representative experiment shown for each cell type, mean ± SEM, $n = 3$.

In PC12 97Q CB_1 cells, Figures 9F and 8B show that the proportion of aggregate-positive cells with 1 μM TFZ was increased by either forskolin (8.0 ± 4.0% increase from veh) or HU210 (6.1 ± 2.6% increase from veh) alone. Unexpectedly, co-treatment using both these compounds in CB_1-transfected cells resulted in a greater than additive, or synergistic, increase in aggregate formation, shifting the aggregate-enhancing effect of HU210 leftwards (data not shown). The combination of forskolin with HU210 increased the proportion of aggregate-positive cells with 1 μM TFZ by 16.7 ± 5.9% compared with vehicle co-treatment (Figure 9F).

Neither functional $G_{i/o}$ nor ERK phosphorylation were required for HU210-mediated enhancement of aggregate formation

We have shown that the rescue of huntingtin-expressing PC12 97Q CB_1 cells by HU210 could be prevented by PTX pretreatment, indicating that $G_{i/o}$ was necessary. Using the same treatment paradigms we next investigated whether there was a requirement for $G_{i/o}$ in the potentiation of aggregate formation by HU210. Figure 10A shows that in both vehicle- and PTX-pretreated PC12 97Q CB_1 cells, there was a concentration-dependent enhancement of aggregate formation by HU210. There was no significant difference in the extent of aggregate potentiation by HU210 between the two pretreatments, either in individual experiments or when data was pooled. Interestingly, there was a trend towards PTX pretreatment enhancing the basal aggregate formation response to induction with 1 μM TFZ. These data indicate that $G_{i/o}$ coupling is not necessary for the CB_1-mediated potentiation of aggregate formation, and that $G_{i/o}$ coupling of other GPCRs in the cell may basally *inhibit* aggregate formation.

ERK 1/2 phosphorylation was not required for HU210-mediated enhancement of aggregate formation. We established that there is a requirement for pERK in the rescue of huntingtin-expressing PC12 97Q CB_1 cells by HU210. We next investigated whether there was a requirement for phosphorylated ERK in the potentiation of aggregate formation by HU210. In PC12 97Q CB_1 cells, pretreatment with the MEK inhibitor, UO126, did not block the potentiation of aggregate formation by HU210, suggesting that this potentiation occurs independently from ERK phosphorylation (Figure 10B). There was no significant difference in the extent of aggregate potentiation by HU210 between vehicle and UO126 pretreatments, either in individual experiments or when data was pooled. However, there was a trend towards UO126 pretreatment enhancing the aggregate formation response with 1 μM HU210 induction. These data indicate that pERK is not necessary for the CB_1-mediated potentiation of aggregate formation, and may even oppose this potentiation.

Discussion and conclusions

We have investigated the ability of cannabinoid agonists to modulate cell death in a cell model of HD, and delineated a mechanism that may underlie the poor neuroprotective efficacy of these compounds in our model and animal studies. We have shown that CB_1 activation was protective against mutant huntingtin-induced cell death, via $G_{i/o}$-mediated inhibition of cAMP, and phosphorylation of ERK. However, CB_1 was also capable of coupling to G_s and the stimulation of cAMP, resulting in enhanced aggregate formation, which was associated with cell death in this system.

Cell survival

PC12 N-terminal huntingtin model of HD. PC12 cells used in this study were sensitive to both truncated wild-type and mutant huntingtin expression. In contrast, application of TFZ to untransfected PC12 cells, or TFZ-induced expression of EGFP alone, was non-toxic (data not shown), suggesting that there was *bona fide* toxicity related to 25Q huntingtin expression. We have previously shown that 25Q huntingtin does not form aggregates (Scotter *et al*., 2008). Steffan *et al*. (2001) have also shown that soluble, truncated, wild-type huntingtin confers toxic properties, enhancing interaction with histone acetyl transferases and dysregulating gene transcription. The exon one wild-type huntingtin 'control' we present here may therefore represent an intermediate HD phenotype, recapitulating the component of toxicity caused by huntingtin truncation but not the component caused by huntingtin aggregation. Un-induced cells may thus be considered a better normal control. However the mutant exon one huntingtin-expressing cell line recapitulates the huntingtin concentration dependence of cell death and aggregate formation in a reproducible fashion, and represents a simplified model for the study of cannabinoids in HD.

HU210 and WIN55212-2 protected against mutant huntingtin toxicity through $G_{i/o}$-mediated inhibition of the cAMP pathway. In these cells we found that HU210 and WIN55212-2, which are full agonists for $G_{\alpha i}$ activation by CB_1 (Glass and Northup, 1999), but not the low-efficacy agonist BAY59-3074 (De Vry *et al*., 2004), conferred protection against mutant, but not 'wildtype', huntingtin-induced cell death. Cannabinoids therefore did not offer significant protection upon the component of toxicity caused by huntingtin truncation. However, comparing death between 'wildtype' and mutant huntingtin-expressing cells it is evident that, despite the absolute level of rescue being small (8%), cannabinoids mitigated most of the aggregation-specific component of toxicity. This protection was receptor-mediated, and agonist concentration-dependent. PTX pretreatment prevented the reduction of huntingtin-induced cell death by HU210, suggesting that protection by HU210 was $G_{i/o}$-dependent.

Transfected PC12 cells used in this study expressed CB_1 receptors at approximately 25 fmol·mg^{-1}. Various studies in human brain show CB_1 receptor levels between approximately 4 and 600 fmol·mg^{-1} (Glass *et al*., 1997; Biegon and Kerman, 2001), demonstrating that the levels in these cells are within the physiological range, and approximate the levels detected autoradiographically in the ventral striatum (33 ± 9 fmol·mg^{-1}; Glass *et al*., 1997).

D1 dopamine receptor agonists and forskolin exacerbated mutant huntingtin toxicity through stimulation of the cAMP pathway. We determined that the inhibition of cAMP via the $G_{i/o}$ G-protein subtypes was critical to the protective potential of CB_1. Supporting this, compounds that enhanced cAMP formation, such as the CB_1 inverse agonist SR141716A, the adenylyl cyclase activator forskolin, and D1 agonists dopamine and SKF38393, exacerbated mutant huntingtin cell death. A detrimental role for both the D1 and forskolin in HD cell survival have been reported previously (Robinson *et al*., 2008). Surprisingly, the D1 antagonist SCH23390 also acted to enhance cell death due to mutant huntingtin, specifically in D1-transfected cells, and particularly at low concentrations. While SCH23390 is highly selective for the D1 receptor, it has been shown to exert D1 agonist-like activity *in vivo* (Wachtel and White, 1995). This agonist activity has been attributed to either low concentrations of SCH23390 or conditions where D2 dopamine receptors are also activated, which may be the case for PC12 cells, which express endogenous D2 and also produce dopamine (Takashima and Koike, 1985).

HU210-mediated rescue of huntingtin-induced cell death is dependent upon pERK. As well as the inhibition of cAMP, we have shown that the phosphorylation of ERK is vital to CB_1-mediated HD cell survival. UO126 pretreatment prevented cellular rescue via CB_1, but did not exacerbate huntingtin cell death in and of itself. Our data suggest that the rapid and transient phosphorylation of ERK following CB_1 activation is necessary but not sufficient for protection against huntingtin cell death. This agrees well with our previous report that showed that the induction of pERK in a majority of cells resulted in activation of the downstream effector EGR-1 (Krox 24) in only a subset of cells, suggesting that additional factors 'gate' the transduction of a pERK response into a particular phenotypic outcome (Graham *et al*., 2006).

Huntingtin aggregate formation
While the mature aggregates detected in our study may not have caused toxicity *per se*, their formation is dependent upon, and therefore a marker of, high concentrations of misfolded soluble monomers/oligomers, which are increasingly being associated with toxicity in a range of neurological diseases (Lambert *et al*., 1998; Watase *et al*., 2002; Caughey and Lansbury, 2003; Walsh and Selkoe, 2004).

HU210 and activators of the cAMP pathway enhanced huntingtin aggregate formation. Having determined a signalling pathway linking CB_1 activation to cell survival in HD, the influence of this pathway on mutant huntingtin aggregate formation was investigated. Cell survival following mutant huntingtin expression was enhanced by the inhibition of cAMP through CB_1, and decreased by the stimulation of cAMP by forskolin or D1 agonists. Therefore it was surprising to find an increase in mutant huntingtin aggregate load following *either* CB_1 activation or the stimulation of cAMP. An HU210-mediated increase in aggregates can be interpreted alone in several ways; the protective effect of HU210 may have allowed cells to survive longer with a large aggregate, hence increasing the proportion of cells with aggregates; HU210 may have exerted protection by driving toxic huntingtin oligomers to form more benign aggregates; or HU210 could have activated both protective and detrimental pathways, resulting in the small magnitude of protection shown in cell survival assays. Alternatively, a simple cause and effect model between aggregate formation and cell death may not be appropriate. These hypotheses and the mechanism for the modulation of aggregate load by HU210 were investigated further.

While CB_1-mediated alleviation of cell death was *Pertussis* toxin sensitive, CB_1-mediated increases in aggregate formation were not. Also, phosphorylated ERK was required for CB_1-mediated alleviation of cell death, but not for CB_1-mediated increases in aggregate load. These findings suggested that different pathways modulated cell survival and aggregate formation with mutant huntingtin expression.

HU210 enhanced huntingtin aggregate formation via G_s. It has been shown that several CB_1 agonists synergise with forskolin in activating G_s (Glass and Felder, 1997; Bonhaus *et al*., 1998). Our finding that HU210 synergized with forskolin in increasing mutant huntingtin aggregate load suggested that CB_1 modulated aggregate formation via G_s coupling. We verified that PTX prevented coupling of CB_1 to the inhibition of cAMP, and unveiled the ability of the receptor to couple to the stimulation of cAMP. However, as this assay measures only net cAMP accumulation, it cannot assess whether, even in the absence of PTX, a proportion of CB_1 receptors may be coupled to G_s. cAMP levels were never completely inhibited to basal levels by HU210, therefore a small subset of CB_1 receptors may feasibly have been stimulating cAMP accumulation even in the absence of PTX. This subset of CB_1 receptors, which, following agonist activation, could stimulate cAMP via G_s, may be responsible for the increase in mutant huntingtin aggregate formation with cannabinoid treatment. In line with this argument, both forskolin and the G_s-coupled D1 dopamine receptor, which stimulate cAMP production, potentiated the formation of mutant huntingtin aggregates. This subset of CB_1 receptors may be those modified by heteromeric interactions with D2 dopamine and/or A2A adenosine receptors, as this has been shown to switch CB_1 signalling from $G_{i/o}$ to G_s both *in vitro* and *in vivo* (Glass and Felder, 1997; Andersson *et al*., 2005; Kearn *et al*., 2005). The transduction of distinct $G_{i/o}$ and G_s signals, rather than a single signal based on the net effect of these G-proteins on cAMP levels, was intriguing. It suggested that there may be compartmentalization of G-proteins, cAMP, and effectors into signalling 'microdomains' in these cells, as has been described in other systems (Houslay, 1995; Daumas *et al*., 2003; Caunt *et al*., 2006). Interestingly, neither WIN55212-2 nor BAY59-3074 increased the formation of mutant huntingtin aggregates. For WIN55212-2 at least, this may be in keeping with the low potency of this ligand for inducing CB_1 coupling to G_s as reported previously (Bonhaus *et al*., 1998).

The extent to which the increase in aggregate formation by CB_1 via G_s influenced the ability of CB_1 to reduce cell death is difficult to determine. However, all other treatments that increased aggregate formation also significantly exacerbated cell death. Our data suggest that a subset of G_s-coupled CB_1 linked HU210 to the increased formation of mutant huntingtin aggregates, and associated toxic consequences, and negated some of the protective effect of the activation of $G_{i/o}$-coupled CB_1 receptors. This phenomenon may underlie the poor neuroprotective efficacy of CB_1 agonists in both this PC12 model and various animal lesion models of HD (Lastres-Becker *et al*., 2003a; de Lago *et al*., 2006). To date there have been no studies published that investigate the efficacy of cannabinoid models in transgenic models of HD.

Our findings in an undifferentiated PC12 cell model of HD support a mechanism for cell-autonomous cannabinoid-mediated neuroprotection, via $G_{i/o}$, and the phosphorylation of ERK. The loss of CB_1 from MSNs early in human HD may therefore exacerbate neuronal pathology. Our data suggest that the synthetic cannabinoid agonist HU210 and WIN55212-2 promoted CB_1 receptors to couple to $G_{i/o}$, attenuating a majority of the component of toxicity associated with huntingtin aggregation; however, HU210 also induced coupling to a competing G_s pathway, which enhanced the formation of aggregates. Promiscuous coupling to these two functionally antagonistic pathways may be a limiting factor in the magnitude of rescue by this cannabinoid. These findings suggest that screening of agonists of fastidious $G_{i/o}$-coupled GPCRs, other CB_1 agonists that promote only $G_{i/o}$ coupling, and/or strategies to prevent the loss of $G_{i/o}$-linked CB_1 signalling may be of therapeutic benefit in HD.

Acknowledgements

This work was supported by a grant from the Marsden Fund of The Royal Society of New Zealand, the Health Research Council of New Zealand and the National Research Centre for Growth and Development. ELS was supported by the Neurological Foundation of New Zealand; ELS and CEG were supported by The University of Auckland. The cell line used in this paper was kindly gifted by Dr Eric Schweitzer (Brain Research Institute, UCLA). Mouse cerebellar tissue was provided by Associate Professor Anthony Hannan (Howard Florey Institute,

Melbourne, Vic., Australia). Dow Agrosciences NZ Ltd. provided the insect steroid hormone TFZ for induction of the cell lines. The authors would also like to thank Dr Hector Monzo and Dr Maurice Curtis for their technical assistance.

Statement of conflicts of interest

The authors declare no conflicts of interest.

References

Aiken CT, Tobin AJ, Schweitzer ES (2004). A cell-based screen for drugs to treat Huntington's disease. *Neurobiol Dis* **16**: 546–555.

Alexander SP, Mathie A, Peters JA (2008). Guide to Receptors and Channels (GRAC), 3rd edition. *Br J Pharmacol* **153**: S1–S209.

Andersson M, Usiello A, Borgkvist A, Pozzi L, Dominguez C, Fienberg AA *et al*. (2005). Cannabinoid action depends on phosphorylation of dopamine- and cAMP-regulated phosphoprotein of 32 kDa at the protein kinase A site in striatal projection neurons. *J Neurosci* **25**: 8432–8438.

Biegon A, Kerman IA (2001). Autoradiographic study of pre- and postnatal distribution of cannabinoid receptors in human brain. *Neuroimage* **14**: 1463–1468.

Bonhaus DW, Chang LK, Kwan J, Martin GR (1998). Dual activation and inhibition of adenylyl cyclase by cannabinoid receptor agonists: evidence for agonist-specific trafficking of intracellular responses. *J Pharmacol Exp Ther* **287**: 884–888.

Caughey B, Lansbury PT (2003). Protofibrils, pores, fibrils, and neurodegeneration: separating the responsible protein aggregates from the innocent bystanders. *Annu Rev Neurosci* **26**: 267–298.

Caunt CJ, Finch AR, Sedgley KR, McArdle CA (2006). Seven-transmembrane receptor signalling and ERK compartmentalization. *Trends Endocrinol Metab* **17**: 276–283.

Charvin D, Vanhoutte P, Pages C, Borrelli E, Caboche J (2005). Unraveling a role for dopamine in Huntington's disease: the dual role of reactive oxygen species and D2 receptor stimulation. *Proc Natl Acad Sci USA* **102**: 12218–12223.

Chen S, Berthelier V, Yang W, Wetzel R (2001). Polyglutamine aggregation behavior *in vitro* supports a recruitment mechanism of cytotoxicity. *J Mol Biol* **311**: 173–182.

Daumas F, Destainville N, Millot C, Lopez A, Dean D, Salome L (2003). Confined diffusion without fences of a G-protein-coupled receptor as revealed by single particle tracking. *Biophys J* **84**: 356–366.

De Vry J, Denzer D, Reissmueller E, Eijckenboom M, Heil M, Meier H *et al*. (2004). 3-[2-cyano-3-(trifluoromethyl)phenoxy]phenyl-4,4,4-trifluoro-1-butanesulfo nate (BAY 59-3074): a novel cannabinoid Cb1/Cb2 receptor partial agonist with antihyperalgesic and antiallodynic effects. *J Pharmacol Exp Ther* **310**: 620–632.

van Dellen A, Blakemore C, Deacon R, York D, Hannan AJ (2000). Delaying the onset of Huntington's in mice. *Nature* **404**: 721–722.

Ebisuya M, Kondoh K, Nishida E (2005). The duration, magnitude and compartmentalization of ERK MAP kinase activity: mechanisms for providing signaling specificity. *J Cell Sci* **118**: 2997–3002.

Ferrante RJ, Kowall NW, Beal MF, Richardson EP Jr, Bird ED, Martin JB (1985). Selective sparing of a class of striatal neurons in Huntington's disease. *Science* **230**: 561–563.

Glass M, Felder CC (1997). Concurrent stimulation of cannabinoid CB1 and dopamine D2 receptors augments cAMP accumulation in striatal neurons: evidence for a Gs linkage to the CB1 receptor. *J Neurosci* **17**: 5327–5333.

Glass M, Northup JK (1999). Agonist selective regulation of G proteins by cannabinoid CB1 and CB2 receptors. *Mol Pharmacol* **56**: 1362–1369.

Glass M, Dragunow M, Faull RL (1997). Cannabinoid receptors in the human brain: a detailed anatomical and quantitative autoradiographic study in the fetal, neonatal and adult human brain. *Neuroscience* **77**: 299–318.

Glass M, Dragunow M, Faull RL (2000). The pattern of neurodegeneration in Huntington's disease: a comparative study of cannabinoid, dopamine, adenosine and GABA(A) receptor alterations in the human basal ganglia in Huntington's disease. *Neuroscience* **97**: 505–519.

Glass M, van Dellen A, Blakemore C, Hannan AJ, Faull RLM (2004). Delayed onset of Huntington's disease in mice in an enriched environment correlates with delayed loss of cannabinoid CB1 receptors. *Neuroscience* **123**: 207–212.

Gonzalez RJ, Tarloff JB (2001). Evaluation of hepatic subcellular fractions for Alamar blue and MTT reductase activity. *Toxicol In Vitro* **15**: 257–259.

Graham ES, Ball N, Scotter EL, Narayan P, Dragunow M, Glass M (2006). Induction of Krox-24 by endogenous cannabinoid type 1 receptors in Neuro2A cells is mediated by the MEK-ERK MAPK pathway and is suppressed by the phosphatidylinositol 3-kinase pathway. *J Biol Chem* **281**: 29085–29095.

Graveland GA, Williams RS, DiFiglia M (1985). Evidence for degenerative and regenerative changes in neostriatal spiny neurons in Huntington's disease. *Science* **227**: 770–773.

Grimsey NL, Narayan PJ, Dragunow M, Glass M (2008). A novel high-throughput assay for the quantitative assessment of receptor trafficking. *Clin Exp Pharmacol Physiol* **35**: 1377–1382.

Hillard CJ, Edgemond WS, Campbell WB (1995). Characterization of ligand binding to the cannabinoid receptor of rat brain membranes using a novel method: application to anandamide. *J Neurochem* **64**: 677–683.

Hoffner G, Island M-L, Djian P (2005). Purification of neuronal inclusions of patients with Huntington's disease reveals a broad range of N-terminal fragments of expanded huntingtin and insoluble polymers. *J Neurochem* **95**: 125–136.

Houslay MD (1995). Compartmentalization of cyclic AMP phosphodiesterases, signalling 'crosstalk', desensitization and the phosphorylation of Gi-2 add cell specific personalization to the control of the levels of the second messenger cyclic AMP. *Adv Enzyme Regul* **35**: 303–338.

Howlett AC, Qualy JM, Khachatrian LL (1986). Involvement of Gi in the inhibition of adenylate cyclase by cannabimimetic drugs. *Mol Pharmacol* **29**: 307–313.

Jin K, LaFevre-Bernt M, Sun Y, Chen S, Gafni J, Crippen D *et al*. (2005). FGF-2 promotes neurogenesis and neuroprotection and prolongs survival in a transgenic mouse model of Huntington's disease. *Proc Natl Acad Sci USA* **102**: 18189–18194.

Kazantsev A, Preisinger E, Dranovsky A, Goldgaber D, Housman D (1999). Insoluble detergent-resistant aggregates form between pathological and nonpathological lengths of polyglutamine in mammalian cells. *Proc Natl Acad Sci USA* **96**: 11404–11409.

Kearn CS, Blake-Palmer K, Daniel E, Mackie K, Glass M (2005). Concurrent stimulation of cannabinoid CB1 and dopamine D2 receptors enhances heterodimer formation: a mechanism for receptor cross-talk? *Mol Pharmacol* **67**: 1697–1704.

Laemmli UK (1970). Cleavage of structural proteins during the assembly of the head of bacteriophage T4. *Nature* **227**: 680–685.

de Lago E, Fernandez-Ruiz J, Ortega-Gutierrez S, Cabranes A, Pryce G, Baker D *et al*. (2006). UCM707, an inhibitor of the anandamide uptake, behaves as a symptom control agent in models of Huntington's disease and multiple sclerosis, but fails to delay/arrest the progression of different motor-related disorders. *Eur Neuropsychopharmacol* **16**: 7–18.

Lambert MP, Barlow AK, Chromy BA, Edwards C, Freed R, Liosatos M *et al*. (1998). Diffusible, nonfibrillar ligands derived from Abeta1-42 are potent central nervous system neurotoxins. *Proc Natl Acad Sci USA* **95**: 6448–6453.

Lastres-Becker I, Bizat N, Boyer F, Hantraye P, Brouillet E, Fernandez-Ruiz J (2003a). Effects of cannabinoids in the rat model of Huntington's disease generated by an intrastriatal injection of malonate. *Neuroreport* **14**: 813–816.

Lastres-Becker I, de Miguel R, De Petrocellis L, Makriyannis A, Di Marzo V, Fernandez-Ruiz J (2003b). Compounds acting at the endocannabinoid and/or endovanilloid systems reduce hyperkinesia in a rat model of Huntington's disease. *J Neurochem* **84**: 1097–1109.

Lehrach H, Wanker EE (2001). Huntington's disease: from gene to potential therapy. *Dialogues Clin Neurosci* **3**: 17–23.

Rasband WS (1997–2009). ImageJ, 1.34s edn. Bethesda, Maryland, USA: U. S. National Institutes of Health [WWW document]. URL http://rsb.info.nih.gov/ij/.

Robinson P, Lebel M, Cyr M (2008). Dopamine D1 receptor-mediated aggregation of N-terminal fragments of mutant huntingtin and cell death in a neuroblastoma cell line. *Neuroscience* **153**: 762–772.

Ross CA, Margolis RL (2001). Huntington's disease. *Clin Neurosci Res* **1**: 142–152.

Saidak Z, Blake-Palmer K, Hay DL, Northup JK, Glass M (2006). Differential activation of G-proteins by mu-opioid receptor agonists. *Br J Pharmacol* **147**: 671–680.

Sanchez I, Mahlke C, Yuan J (2003). Pivotal role of oligomerization in expanded polyglutamine neurodegenerative disorders. *Nature* **421**: 373–379.

Scherzinger E, Sittler A, Schweiger K, Heiser V, Lurz R, Hasenbank R *et al*. (1999). Self-assembly of polyglutamine-containing huntingtin fragments into amyloid-like fibrils: implications for Huntington's disease pathology. *Proc Natl Acad Sci USA* **96**: 4604–4609.

Scotter EL, Narayan P, Glass M, Dragunow M (2008). High throughput quantification of mutant huntingtin aggregates. *J Neurosci Methods* **171**: 174–179.

Spires TL, Grote HE, Varshney NK, Cordery PM, van Dellen A, Blakemore C *et al*. (2004). Environmental enrichment rescues protein deficits in a mouse model of Huntington's disease, indicating a possible disease mechanism. *J Neurosci* **24**: 2270–2276.

Steffan JS, Bodai L, Pallos J, Poelman M, McCampbell A, Apostol BL *et al*. (2001). Histone deacetylase inhibitors arrest polyglutamine-dependent neurodegeneration in Drosophila. *Nature* **413**: 739–743.

Suhr ST, Gil EB, Senut MC, Gage FH (1998). High level transactivation by a modified Bombyx ecdysone receptor in mammalian cells without exogenous retinoid X receptor. *Proc Natl Acad Sci USA* **95**: 7999–8004.

Takashima A, Koike T (1985). Relationship between dopamine content and its secretion in PC12 cells as a function of cell growth. *Biochim Biophys Acta* **847**: 101–107.

Wachtel SR, White FJ (1995). The dopamine D1 receptor antagonist SCH 23390 can exert D1 agonist-like effects on rat nucleus accumbens neurons. *Neurosci Lett* **199**: 13–16.

Walsh DM, Selkoe DJ (2004). Oligomers on the brain: the emerging role of soluble protein aggregates in neurodegeneration. *Protein Pept Lett* **11**: 213–228.

Watase K, Weeber EJ, Xu B, Antalffy B, Yuva-Paylor L, Hashimoto K *et al*. (2002). A long CAG repeat in the mouse Sca1 locus replicates SCA1 features and reveals the impact of protein solubility on selective neurodegeneration. *Neuron* **34**: 905–919.